Nodulisporic Acid Opens Insect Glutamate-Gated Chloride Channels: Identification of a New High Affinity Modulator

McHardy M. Smith,*,‡ Vivien A. Warren,‡ Brande S. Thomas,‡ Richard M. Brochu,‡ Eric A. Ertel,‡,§ Susan Rohrer,|| James Schaeffer,|| Dennis Schmatz,⊥ Brian R. Petuch,# Yui Sing Tang,▽ Peter T. Meinke,▼ Gregory J. Kaczorowski,‡ and Charles J. Cohen‡

Department of Membrane Biochemistry and Biophysics, Department of Endocrinology and Chemical Biology, Department of Basic Animal Sciences Research, Natural Products Drug Discovery, Department of Drug Metabolism, and Department of Basic Medicinal Chemistry, Merck Research Laboratories, RY80C31N, P.O. Box 2000, Rahway, New Jersey 07065-0900

Received December 23, 1999; Revised Manuscript Received March 2, 2000

ABSTRACT: Nodulisporic acid (NA) is an indole diterpene fungal product with insecticidal activity. NA activates a glutamate-gated chloride channel (GluCl) in grasshopper neurons and potentiates channel opening by glutamate. The endectocide ivermectin (IVM) induces a similar, but larger current than NA. Using *Drosophila melanogaster* head membranes, a high affinity binding site for NA was identified. Equilibrium binding studies show that an amide analogue, *N*-(2-hydroxyethyl-2,2-^{3}H)nodulisporamide ([^{3}H]NAmide), binds to a single population of sites in head membranes with a K_D of 12 pM and a B_{max} of 1.4 pmol/mg of protein. A similar K_D is determined from the kinetics of ligand binding and dissociation. Four lines of evidence indicate that the binding site is a GluCl. First, NA potentiates opening of a glutamate-gated chloride current in grasshopper neurons. Second, glutamate inhibits the binding of [^{3}H]NAmide by increasing the rate of dissociation 3-fold. Third, IVM potently inhibits the binding of [^{3}H]NAmide and IVM binds to GluCls. Finally, the binding of [^{3}H]IVM is inhibited by NA. The B_{max} of [^{3}H]IVM is twice that of [^{3}H]NAmide, and about half of the [^{3}H]IVM binding sites are inhibited by NA with high affinity (K_I = 25 pM). In contrast, [^{3}H]IVM binding to *Caenorhabditis elegans* membranes is not inhibited by NA at 100 nM, and there are no high affinity binding sites for NA on these membranes. Thus, half of the *Drosophila* IVM receptors and all of the NA receptors are associated with GluCl. NA distinguishes between nematode and insect GluCls and identifies subpopulations of IVM binding sites.

Ligand-gated ion channels form a collection of supramolecular complexes that are intimately involved in synaptic transmission. One class of these channels is the glutamate-gated chloride channels (GluCl); this family has been identified in invertebrates and is the target for the avermectins (*1*). The avermectins and milbemycins, represented by the semisynthetic ivermectin (IVM),[1] are macrocyclic lactones and are used broadly in animal and human health, and crop protection (*2, 3*). Based on studies with the nematode *Caenorhabditis elegans*, the anthelmintic and insecticidal activity of IVM has been ascribed to its ability to bind to and open GluCls, either alone or by potentiating the effect of glutamate (*4*−*7*). A receptor for IVM in *C. elegans* was identified by expression cloning (*7*). Coexpression of an α-subunit and a *β*-subunit of this receptor reconstitutes a channel gated by glutamate and IVM. Subsequently, two additional α-subunits were identified in *C. elegans* (*8, 9*). Elimination of all three α-subunits eliminates high affinity binding sites for [^{3}H]IVM and confers 4000-fold resistance to this anthelmintic (*9*). In the insect *Drosophila melanogaster*, high affinity binding has been reported (*10*), and an IVM-sensitive GluCl homologue has been cloned (*11*). In insects, the nature of ivermectin binding sites and the mechanism of action are less well-defined, and several studies suggest that ivermectin may have at least one other target beyond GluCl: evidence exists for an interaction of IVM with GABA-gated chloride channels in both nematodes (*12*−*14*) and insects (*15, 16*).

We now report studies with a newly discovered compound, nodulisporic acid (NA), which demonstrate that IVM binds to multiple receptors in insects, as has been found for IVM with *C. elegans* (*9*). Nodulisporic acid (NA, Scheme 1), a novel indole diterpene, was isolated from cultures of an endophytic fungus *Nodulisporium* sp. (*17*) based on insecticidal activity (*18*). The molecule has no gross structural similarity to IVM, and the mechanism of NA insecticidal activity had not been identified. Indole diterpenes are known to be potent insecticides (*19, 20*); some are also allosteric activators of vertebrate GABA-A receptors (*21*) or blockers

* To whom correspondence should be addressed at Merck Research Laboratories, RY80N-31C, P.O. Box 2000, Rahway, NJ 07065. Voice: 732-594-7013; Fax: 732-594-3925; E-mail: mchardy_smith@merck.com.

‡ Department of Membrane Biochemistry and Biophysics.

§ Present address: F. Hoffmann−La Roche, 70/426, Postfach, CH-4070 Basel, Switzerland.

|| Department of Endocrinology and Chemical Biology.

⊥ Department of Basic Animal Sciences Research.

Natural Products Drug Discovery.

▽ Department of Drug Metabolism.

▼ Department of Basic Medicinal Chemistry.

[1] Abbreviations: GABA, γ-aminobutyric acid; HEPES, *N*-(2-hydroxyethyl)piperazine-*N*′-2-ethanesulfonic acid; IVM, ivermectin; NA, nodulisporic acid; NAmide, *N*-(2-hydroxyethyl)nodulisporamide; [^{3}H]-NAmide, *N*-(2-hydroxyethyl-2,2-^{3}H)nodulisporamide.

10.1021/bi992943i CCC: $19.00
Published on Web 04/13/2000

Scheme 1: Structure of Nodulisporic Acid (NA) and Synthetic Scheme for NAmide and [^{3}H]NAmide[a]

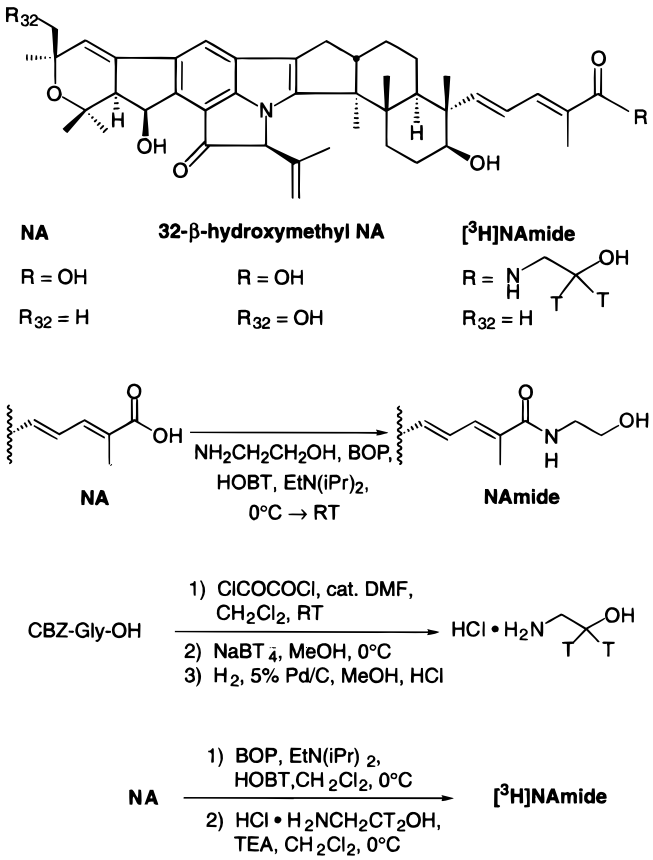

[a]32-β-Hydroxymethyl NA is biologically inactive in insecticidal assays. In the scheme, CBZ = carbobenzyloxy, HOBT = *N*-hydroxybenzotriazole, and BOP = benzotriazol-1-yloxytris(dimethylamino)-phosphonium hexafluorophosphate.

of large conductance Ca^{2+}-activated potassium (Maxi-K) channels (*22*). We demonstrate that the mechanisms of action of NA and IVM on insect GluCl are similar.

To identify the mechanism of action of NA, two experimental approaches were used: whole cell electrophysiological recordings of grasshopper neurons and radioligand binding to membrane preparations from *D. melanogaster* heads. Grasshopper motorneurons are amenable to whole cell voltage clamp studies, and the soma have a variety of voltage and ligand-gated ion channels (*23*−*26*). Ligand binding studies were performed with *D. melanogaster* head membranes because this is a convenient preparation for obtaining the larger quantities of membranes used in ligand binding studies for characterizing insect neuronal receptors. Electrophysiological studies show that NA activates a glutamate-gated chloride channel and potentiates channel opening by glutamate. In *Drosophila* head membranes, a high affinity binding site for an amide derivative of NA was identified. Binding to this site is allosterically inhibited by glutamate and is coupled to an IVM binding site. Thus, both electrophysiological and ligand binding studies indicate that NA modulates insect glutamate-gated chloride channels.

MATERIALS AND METHODS

Materials. Ibotenate was from Biomol Research Labs (Plymouth Meeting, PA), and muscimol was from Tocris Cookson (Langford, Bristol, U.K.). All HEPES buffer stock solutions (1 M) were adjusted to a pH of 7.5 using KOH and used without further pH adjustment. IVM and IVM-PO_4 were from the Merck sample collection; [^{3}H]IVM, at 44 Ci/mmol, was synthesized by the Drug Metabolism group, Merck Research Laboratories, Rahway, NJ. NA was isolated as per (*17*).

Synthetic Methods. To synthesize NAmide: to nodulisporic acid (200 mg) in CH_2Cl_2 (20 mL) at 0 °C were added sequentially $NH_2CH_2CH_2OH$ (92 μL), *N*-hydroxybenzotriazole (40 mg), and $EtN(iPr)_2$ (178 μL) followed by benzotriazol-1-yloxytris(dimethylamino)phosphonium hexafluorophosphate (224 mg) (Scheme 1). The cooling bath was removed, and the solution was incubated at room temperature for 2 h. The solution was then poured into brine/water (1/1), acidified to pH ~4 using glacial HOAc, extracted with CH_2Cl_2, and dried (Na_2SO_4). The solution was filtered, and volatiles were removed under reduced pressure. Pure product (187 mg, 87%) was obtained following flash chromatography on silica gel using gradient elution (4/96 → 7/93 → 10/90 of 10% NH_4OH solution in MeOH/$CHCl_3$ as eluant). By TLC, the product had an $R_f = 0.31$ (10/90 of 10% NH_4OH solution in MeOH/$CHCl_3$ as eluant). By HPLC, the product had a $t_R = 5.98$ min (1.5 mL/min, 55/45 MeCN/H_2O, Zorbax RX-8 column, 15 cm × 4 mm). By MS, the product had *m*/*z* 723.4 (M^++H). NMR: (500 MHz, $CDCl_3$) δ 7.71 (s, 1H), 7.03 (d, $J = 10.3$ Hz, 1H), 6.36 (dd, $J_1 = 11.2$ Hz, $J_2 = 15.1$ Hz, 1H), 6.25 (br t, 1H), 6.06 (d, $J = 2.7$ Hz, 1H), 5.82 (d, $J = 15.4$ Hz, 1H), 5.26 (d, $J = 6.4$ Hz, 1H), 5.21 (s, 1H), 5.09 (s, 1H), 5.01 (br s, 1H), 3.80 (t, $J = 4.6$ Hz, 2H), 3.54 (dd, $J_1 = 5.0$ Hz, $J_2 = 10.2$ Hz, 2H), 3.41 (br s, 1H), 2.89 (dd, $J_1 = 6.0$ Hz, $J_2 = 2.8$ Hz, 1H), 2.85 (br s, 1H), 2.75 (dd, $J_1 = 6.5$ Hz, $J_2 = 14.0$ Hz, 1H), 2.65 (s, 1H), 2.33 (t, $J = 9.0$ Hz, 1H), 2.01 (s, 3H), 1.51 (s, 3H), 1.37 (s, 3H), 1.36 (s, 3H), 1.27 (s, 3H), 1.16 (s, 3H), 1.15 (s, 3H), 1.07 (s, 3H), 0.97 (s, 3H).

[^{3}H]NAmide (*N*-(2-hydroxyethyl-2,2-^{3}H)nodulisporamide, Scheme 1) was synthesized as follows: *n*-protected glycine was converted into the corresponding acid chloride using oxallyl chloride. Treatment of CBZ-Gly-Cl with sodium borotritide yielded, following reversed-phase HPLC purification, pure CBZ-$HNCH_2CT_2OH$. The CBZ group was removed by hydrogenation and the $HCl{\cdot}H_2NCH_2CT_2OH$ coupled under standard conditions with the active ester of nodulisporic acid, producing [^{3}H]NAmide at a specific activity of 22 Ci/mmol (Scheme 1).

32β-Hydroxymethyl NA was generated by biotransformation of NA during culture with *Streptomyces* sp. (Merck culture strain MA 6966). Biotransformation products were extracted from the culture medium, purified by HPLC, and subjected to electrospray MS and NMR to establish structure. In addition to isolating and identifying the structure and biological activity of 32β-hydroxymethyl NA, the 31α-hydroxymethyl NA derivative was also generated.

Electrophysiological Recordings. The procedure for isolating soma of grasshopper thoracic neurons was similar to that described by Suter and Usherwood (*27*) except that neurons were isolated from both the metathoracic and the mesothoracic ganglia and mechanical disruption of the ganglia was more extensive in order to obtain cell surfaces suitable for gigaohm seal formation. No enzymes were used to establish the primary cultures. Voltage-clamp studies were conducted with the whole cell voltage clamp technique using a Dagan

3900A amplifier (Dagan Instruments, Minneapolis, MN). Data were acquired using the program Pulse, and most analysis was performed with the companion program Pulsefit (Instrutech Instruments, Great Neck, NY). The internal (pipet) solution usually contained (in mM): CsF, 113; CsCl, 20; $CaCl_2$, 0.9; $MgCl_2$, 1; HEPES, 20; 1,2-bis(2-aminophenoxy)ethane-*N*,*N*,*N*′,*N*′-tetraacetic acid (BAPTA), 11, pH 7.2 with CsOH. The external solution contained (in mM): NaCl, 150; $CaCl_2$, 1.8; $MgCl_2$, 0.5; HEPES, 10, pH 7.5 with NaOH. In some experiments, the pipet solution also contained 5 mM Mg-ATP and 0.1 mM Li_2-GTP, and the bath solution contained 161 mM NaCl and 4 mM KCl (grasshopper saline). All experiments were conducted at room temperature (20−25 °C). Low Cl solutions contained sodium methanesulfonate in place of NaCl. Drugs were typically diluted at least 1000-fold from dimethyl sulfoxide stock solutions.

Insecticidal Assays. Test agents were injected into adult grasshoppers weighing about 2 g. The vehicle was 11% dimethyl sulfoxide in grasshopper saline. The drug concentration was adjusted so that 5 μL of test solution was injected.

Binding Assays. D. melanogaster (Oregon R) were cultured by standard techniques, and adults were harvested and stored frozen at −70 °C until membrane preparation. The heads were broken off the bodies by vigorous shaking while the flies were frozen. Sieving separated the heads (and legs) from the bodies. Heads derived from 5 g of whole flies (ca. 20 mL of loosely packed flies) were homogenized in 20 mL of ice-cold 10 mM HEPES by two 5 s bursts at a power setting of 5 with a Brinkmann Polytron. The homogenate was poured through two layers of cotton gauze and then subjected to centrifugation for 5 min at 500*g*. The supernatant was decanted and subjected to centrifugation at 20000*g* for 15 min. The resulting high-speed pellet was either resuspended in 20 mL of 50 mM HEPES to make a solution of approximately 1 mg of membrane protein/mL, which was used immediately, or flash-frozen in liquid N_2 and stored at −70 °C. Alternatively, the pellet was resuspended in 2 mL of 10 mM HEPES and loaded on a sucrose step gradient composed of 2 mL steps of 12%, 24%, 36%, 48%, and 60% sucrose (w/w), all in 50 mM HEPES. The gradient was subjected to centrifugation at 40 000 rpm in a Beckman SW40 rotor for 1 h, and then the interfaces were drawn off and used immediately or stored at −70 °C for later use.

For *Lucilia sericata* and *Musca domestica*, heads were separated from other body parts by floating on liquid N_2, and heads were carried through the above homogenization and centrifugation procedure. Lepidopterians, grasshopper heads, legs, ganglia, and larval stages of *D. melanogaster* were homogenized using a Brinkmann Polytron and carried through the above three centrifugation steps. *C. elegans* membranes were prepared as described (*4*, *28*). Fresh brain from rat was used as starting material for purification of synaptic plasmalemmal membranes (*29*).

Binding of [^{3}H]NAmide and [^{3}H]IVM were measured using a modification of a binding assay described previously (*4*, *10*). This protocol was followed: 10 μg of membrane protein was incubated for various times, usually 3 h to overnight, in borosilicate tubes with radioactive ligand, with or without test compound, in 0.1−10 mL final volume (usually 1−5 mL; initial experiments were at lower volumes, and as the true affinity was recognized, incubation times and volumes were increased to accommodate lower receptor concentrations and complete ligand equilibration) in a medium composed of 50 mM HEPES, pH 7.5 with KOH, 0.1 mg/mL bacitracin, and 2% dimethyl sulfoxide, at room temperature. The binding reaction was terminated, and bound ligand was separated from free ligand by addition of 3 mL of an ice-cold wash solution composed of 0.5% Triton followed rapidly by filtration though Whatman GF/C glass fiber filters under reduced pressure. The filters had been prewetted with 0.15% Triton X-100 and 0.25% polyethylenimine. Filters were washed twice with 3 mL of 0.5% Triton X-100, and then radioligand trapping was assessed by liquid scintillation techniques. Samples were normally analyzed until the 2 sigma counting error was less than 2%, or 5 min counting time (whichever was reached first), for usually 6 times or more, and the average CPM was calculated from the multiple counts available; replicate samples seldom varied by more than 3%.

The important modifications to the prior protocol (*4*, *10*) were the addition of bacitracin, the increase in the incubation time from 1 h to overnight and in the assay volume from 1 to 3 mL, and the reduction of the membrane concentration from 50 to 10 μg of protein/assay tube. In the absence of bacitracin and without membrane protein, less that 10% of added radioligand, either [^{3}H]NAmide or [^{3}H]IVM, was freely removable from the assay tube 1 h after addition, whereas with bacitracin, at concentrations ranging from 10 μg/mL to 1 mg/mL, greater than 90% of added radioligand was removable from the assay tube 1 h after addition. Thus, bacitracin was added constitutively to ensure that added radioligand closely approximated free radioligand. The second two crucial modifications were to increase incubation times and volumes to allow receptor and ligand to come to equilibrium. Finally, by decreasing membrane protein and increasing assay volume, we tried to maintain receptor concentration at one-fifth of K_D or below, although some initial experiments were done at K_D (e.g., Figures 5A and 7) or higher receptor concentration (e.g., Figures 4, 5B, and 6); in cases where total receptor concentration is substantially above K_D, one must be vigilant that one is not merely titrating receptor and thereby not obtaining correct K_D and K_I values (this effect may have increased K_I values ca. 2-fold for the results shown in Figure 6).

Data were graphed and fitted to equations using Igor Pro (Wavemetrics, Lake Oswego, OR). Specific binding is defined as total binding (that seen in the absence of competitor) minus nonspecifically associated ligand (binding seen in the presence of a high concentration of competitor). In saturation binding isotherm experiments, nonspecific binding was fit to a linear regression, and then total binding was fit to

$$B = B_{max}L/(K_D + L) + NSL + CB$$

where B is the amount bound, B_{max} is the maximal number of binding sites, L is the free ligand concentration, K_D is the equilibrium dissociation constant, NS is the slope of the nonspecific binding component, and CB is the counter background; the NS and CB parameters were fixed at those found for nonspecific binding. When specific binding was analyzed, the NSL + CB component was removed from the equation. These equations have an implicit Hill coefficient of 1.

The pseudo-first-order rate constant for the binding reaction, k_{obs}, was determined by plotting the specific binding as a function of time and fitting those data to a monoexponential function. k_{obs} was converted into the second-order rate constant of association by plotting k_{obs} vs [ligand], and fitting the data by linear regression. From the slope and intercept of that line, through the relationship:

$$k_{obs} = k_1[[^3H]\text{NAmide}] + k_{-1}$$

we determined k_1 and k_{-1}. This equation assumes infinite receptor dilution, which is likely not to be true. The rate constant of dissociation, k_{-1}, was also determined from plotting specific binding vs time as a monoexponential relationship. Inhibition curves were fit by pooling data from multiple experiments as fractional specific binding at each concentration of competitor, and modeling the resulting data by the equation:

$$\text{fraction bound} = 1 - [S/(S + IC_{50})]$$

where S is the concentration of competitor and IC_{50} is the IC_{50} value for the potency of the inhibition. IC_{50} can be corrected to K_I by the relationship:

$$K_I = IC_{50}/[1 + (L/K_D)]$$

where L, IC_{50}, and K_D have the definitions above. As well, when one varies ligand concentration, while keeping inhibitor concentration constant, the K_I for inhibitor [S] is determined by a similar equation:

$$K_I = [S]/[(\text{“}K_D\text{”}/K_D) - 1]$$

where “K_D” is equal to the K_D in the presence of inhibitor [S]. In Figure 6B, in which a two-component model is used, the equation used to model the data is

$$\text{fraction bound} = 1 - [(B_H S)/(S + K_H) + ((1 - B_H)S)/(S + K_L)]$$

where K_H and K_L are the IC_{50} values for inhibition at the high and low affinity binding sites, respectively, and B_H is the fraction of binding sites with high affinity for the competitor. When fitting, data points were weighted by the inverse of the standard deviation of the replicates.

RESULTS

Functional Effects of NA on Grasshopper Neurons. Glutamate-gated chloride channels were first described in grasshoppers (*30*), and the thoracic ganglia have a high density of IVM binding sites (*10*). Nodulisporic acid (NA) induces a large steady-state current in the soma of motorneurons isolated from these ganglia (Figure 1A,C,D). The NA-induced current linearly changes with voltage and reverses at ≈−50 mV (Figure 1A). Reducing extracellular [Cl^-] from 154 to 5 mM by replacement with methanesulfonate shifts the reversal potential to ≈−25 mV and reduces both inward and outward current. Ivermectin phosphate (IVM-PO_4) induces a similar Cl-sensitive current in these neurons (Figure 1B). The similarity between the currents induced by NA and IVM and the known activity of IVM on glutamate-gated Cl channels (*7, 11*) suggest that NA might also activate a GluCl. We tested for this mechanism by applying NA in combination with either glutamate or IVM.

Co-application of NA and glutamate indicates an interaction between these two agonists (Figure 1C). Bath application of a low concentration of glutamate elicited a small current (bath application underestimates the maximal GluCl current as these channels rapidly desensitize). The neuron was then exposed to 0.1 μM NA, which caused a small, steady opening (not shown). Increasing the concentration of NA to 0.3 μM elicited a much larger current that desensitized and deactivated very slowly. After exposure to NA, reapplication of the same concentration of glutamate elicited a much larger current that desensitized much more slowly than prior to NA application. This potentiation of the glutamate effect indicates that NA and glutamate modify the same channel and indicates that NA may be an allosteric modulator of GluCl channels. Similar interactions between NA and glutamate were observed in three experiments.

We tested whether NA and IVM-PO_4 act on the same channel by co-applying these insecticides (Figure 1D). The left trace shows activation of a current by NA at 50 nM and 1 μM. Other studies demonstrated that 1 μM NA is a maximally effective concentration; 100 and 300 nM NA elicited currents 36 ± 5% and 84 ± 1% (±SEM, $n = 4$) of that caused by 1 μM NA. Subsequent addition of IVM caused much greater channel activation. In contrast, NA never induced additional current when IVM was applied first, as shown in the right panel of Figure 1D. These studies suggest that native insect neurons contain two populations of IVM-sensitive chloride channels: one of which is also activated by NA and another that is not. Alternatively, NA could be a partial agonist, but results below argue against that hypothesis.

The electrophysiological results predict that NA has insecticidal activity similar to IVM. This was demonstrated by direct injection into adult grasshoppers. The minimal effective dose for killing grasshoppers of NA and IVM is 0.5 and 5 nmol, respectively. In contrast to pyrethroids, which produce a rapid “knock down”, both NA and IVM cause gradual paralysis and death after about 18 h. An analogue of NA, NA D (*17*), is inactive in the binding studies described below and also inactive in this insecticidal assay at 5 nmol.

Specificity of NA Action. NA is a very hydrophobic molecule and, as such, could be acting on the grasshopper GluCl as a nonspecific membrane perturbant. If so, then it would likely disrupt interactions at a large number of vertebrate receptors and ion channels. To determine the selectivity of NA, this agent was tested at 10 μM in 108 receptor ligand binding and enzymatic assays in a standard PanLabs screen. There was no significant interaction (≥30% inhibition) with any of these targets, except for modest inhibition of ligand binding to thromboxane A_2, glucocorticoid, and muscarinic M_3 receptors (45, 39, and 38% inhibition, respectively). The concentration used in the specificity tests is 10-fold higher than the maximally effective concentration of NA needed to activate glutamate-gated chloride channels in grasshopper neurons. NA had little or no effect in various other binding assays using a number of membrane-bound neurotransmitter or hormone receptors, or in enzyme assays measuring kinase, phosphastase, or syn-

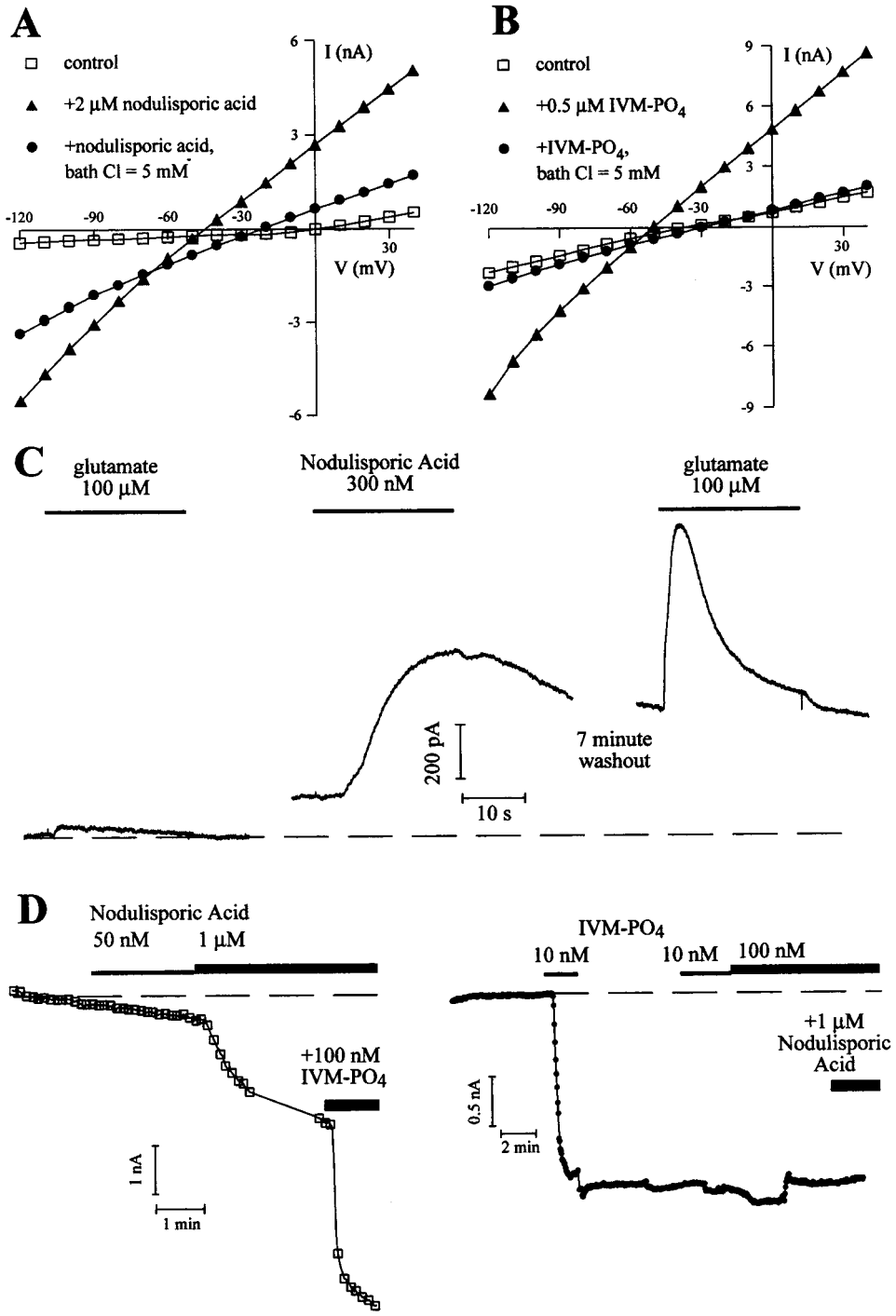

FIGURE 1: Chloride currents activated by NA or ivermectin in grasshopper motorneurons. (A and B) Steady-state current−voltage relationship for conductance induced by NA (A) or by IVM-PO_4 (B). Each symbol indicates the average current measured at the end of a 200 ms step to the indicated voltage. Control before drug addition (bath chloride of 160 mM, □); with 2 μM NA (A, ▲) or 0.5 μM IVM-PO_4 (B, ▲); in drug after reducing bath chloride to 5 mM by equimolar replacement with methanesulfonate (●). (C) NA potentiates a glutamate-induced chloride current. The three traces shown were recorded successively from a grasshopper motorneuron; holding potential = 0 mV. The dashed line indicates the holding current before application of NA or glutamate. Bath application of 100 μM glutamate elicited a small current. 100 nM NA induced a small maintained current (not shown). Increasing NA to 300 nM (indicated by the bar) increased the outward current. This current did not deactivate even after 7 min of washing. Reapplication of 100 μM glutamate elicited a larger current after exposure to NA. (D) Current induced by co-application of NA and IVM-PO_4. The neurons were clamped at −60 mV (near the reversal potential for chloride), and the holding current is indicated by a dashed line. A 200 ms pulse to −120 mV was applied at 0.5 Hz, and the symbols indicate the mean current measured at the end of this voltage step. Left panel: NA activates an inward current. 100 nM IVM-PO_4 was added 3 min after adding 1 μM NA and caused further current activation. Right panel: In contrast, NA did not activate additional current in the presence of 100 nM IVM-PO_4. Metathoracic neurons, 25−35 μm in diameter.

thetase activities. Ion channels, both ligand-gated (i.e., nicotinic, $GABA_A$, $GABA_B$, glutamate-NMDA, glutamate-AMPA, glycine) and voltage-gated (i.e., Brain IIA sodium, N-type calcium, K_V1.X potassium, K-ATP potassium, and calcium-activated potassium) channels, were also examined. A weak interaction with L-type calcium channels (25% inhibition of [^{3}H]nitrendipine binding, but no effect on [^{3}H]-diltiazem binding) was observed at 10 μM NA. Using rat

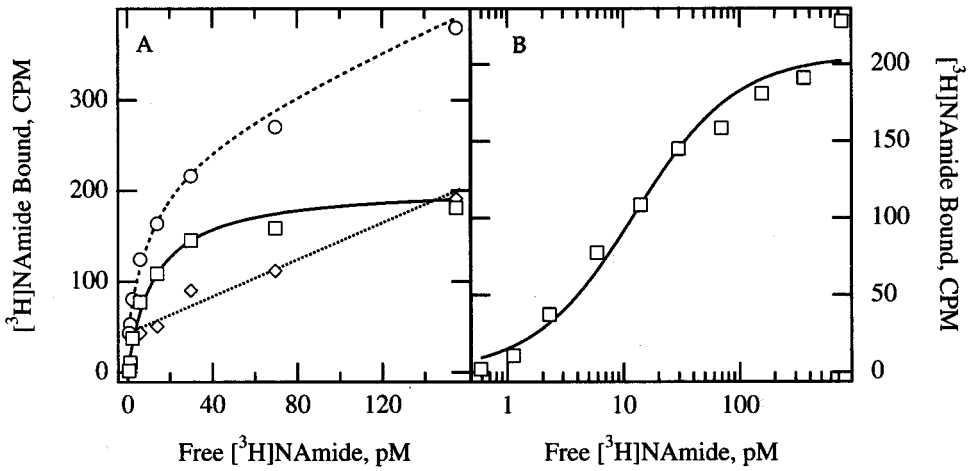

FIGURE 2: [^{3}H]NAmide identifies a high affinity binding site in *D. melanogaster* head membranes. Panel A: Total binding of [^{3}H]NAmide to fly head membranes was assayed in 5 mL (○), and nonspecific retention of radioactivity on the filter was assessed in the presence of 0.3 μM competing NA (◇); specific binding was calculated by subtracting nonspecific binding from total binding (□). The data were fit to models, as described under Materials and Methods: a linear regression of the nonspecific retention of [^{3}H]NAmide, or for binding in the absence of competing NA, is fit to a model of a single binding site showing no cooperativity (an implicit Hill coefficient of 1) with (○), or without (□), an allowance for a contribution of nonspecific binding. Panel B: Specific binding in panel A was replotted on a log scale (including two points at higher concentrations, not shown in panel A); the line is a nonlinear curve fit to a population of receptors with a single affinity for the receptor. The affinity calculated was 12.5 pM, and the B_{max} estimate was 205 CPM/assay tube or 1.6 pmol/mg of protein; the receptor concentration in this assay was 1.63 pM.

brain poly A mRNA injected into oocytes, 2 μM NA had no discernible effect on expressed Na or K channel function. However, in patch voltage clamp experiments, 0.1 μM NA causes 50% inhibition of high-conductance, calcium-activated potassium (Maxi-K) channels in bovine aortic smooth muscle cells. The inhibition of this channel is not unexpected since Maxi-K channels are known to be inhibited by indole diterpenes (*22*). However, NA is 10−100-fold weaker as a channel blocker than the previously identified indole diterpines, paxilline, aflatrem, and paspalatrem (*22*). As a final indicator of the specificity of NA, a relatively high concentration of NA was applied to many different central nervous system channels and receptors, and changes in behavioral output were observed. Two micrograms of NA was administered by intracranial injection into weanling female rats; no signs of behavioral abnormalities or toxicity were observed after 30 min ($n = 4$). For comparison, intracranial injection of 1 μg of the selective, small-molecule K_V1.X inhibitor, correolide (*31*), or 10 ng of the selective peptide inhibitor of K_v1.1, -1.2, and -1.3 channels, margatoxin (*32*), produced ataxia, writhing, and tonic seizures within 5−10 min ($n = 2$ each); the animals were euthanized immediately thereafter. By this criterion, NA displays no significant neuronal toxicity in mammals. The lack of effect on so many mammalian channels and receptors indicates that NA is not just a nonspecific membrane perturbant.

NA Binds with High Affinity to Membranes from D. melanogaster Heads. A tritiated amide derivative of NA, [^{3}H]-NAmide (Scheme 1), was used to identify high affinity binding sites in *D. melanogaster* head membranes. Equilibrium binding of this ligand to its receptor was characterized by incubating overnight increasing concentrations of [^{3}H]-NAmide with purified membranes; binding in the presence of 0.3 μM NA or 0.1 μM IVM (see below) was defined as nonspecific and subtracted from total binding to obtain specific binding. Under the conditions specified under Materials and Methods, nonspecific binding is linearly related to free [^{3}H]NAmide (Figure 2A). Specific binding is well described by a fit to a single population of binding sites with a dissociation constant (K_D) of 12.5 pM (Figure 2A,B).

The binding of [^{3}H]NAmide to fly head membranes is rapid and reversible. Figure 3A shows the rate of association of three concentrations of [^{3}H]NAmide to its binding site. The rate of binding increased with ligand concentration as expected for a 1 to 1 binding reaction, and the association rate constant ($k_1 = 2.53 \times 10^7$ M^{-1} s^{-1}, Figure 3B) is consistent with that expected for aqueous diffusion rates. To determine the reversibility of [^{3}H]NAmide binding, membranes were equilibrated with [^{3}H]NAmide for 40 min, and then 0.3 μM NA was added. The amount of [^{3}H]NAmide associated with the membranes declined monoexponentially with an off rate (k_{-1}) of 0.00035 s^{-1} (Figure 3, see also Figure 5); on average, $k_{-1} = 0.00020 \pm 0.00003$ s^{-1} with a half-time of 57 ± 7 min (SEM, $n = 14$). For the experiment shown, the K_D calculated from the ratio of the association and dissociation rates was 12.05 pM, in good agreement with equilibrium measurement of the K_D (12.5 pM, Figure 2). This suggests that association of [^{3}H]NAmide with membranes is to a population of high affinity receptor sites with one affinity or multiple populations of receptors with very similar affinities (*33*).

The NA and IVM Binding Sites Co-sediment. D. melanogaster head membranes also have high affinity binding sites for [^{3}H]IVM (*10*). Thus, we investigated whether the binding sites for [^{3}H]NAmide co-localize with the [^{3}H]IVM receptor. Membrane fractions were obtained from discontinuous sucrose gradients, and the fractions across the gradient were assessed for specific binding of [^{3}H]IVM and [^{3}H]NAmide (Figure 4). Ligand concentration was greater than 5-fold over K_D for both receptors; therefore, both receptors are near saturation. Near complete recovery of all binding activity for both ligands is achieved. The binding sites co-localize at the 24/36% sucrose interface. Binding of [^{3}H]saxitoxin, a ligand for Na^+ channels, localizes to an equivalent region of the gradient (data not shown), indicating that the mem-

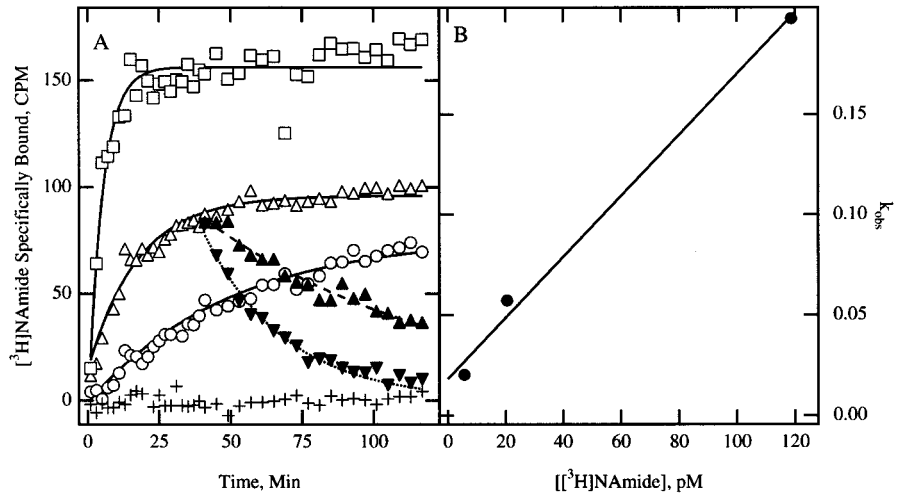

FIGURE 3: Kinetics of association and dissociation of [^{3}H]NAmide to receptors in *D. melanogaster* head membranes. Panel A: Equal amounts of membranes were incubated for varying periods of time with three different concentrations of [^{3}H]NAmide (118 pM, □; 21 pM, △; and 6 pM, ○; in respectively 2 mL, 5 mL, and 10 mL assay volumes). To additional samples at 21 pM [^{3}H]NAmide was added NA at 40 min (▲) to a final concentration of 0.3 μM, or 0.1 mM ibotenate and 0.3 μM NA were added together (▼) and samples were taken at the indicated times for the determination of the remaining [^{3}H]NAmide bound. Nonspecific retention of [^{3}H]NAmide (+) equilibrated immediately to an average of 42.85 CPM per assay point (±2.80 CPM, SD = 2.8, n = 39; which included a filter blank of 34.2 ± 1.3 CPM, n = 3), and the nonspecific retention value has been subtracted from all of the values plotted above. Panel B: The observed rate of association (k_{obs}) modeled from the data in the left panel was replotted in panel B versus the concentration of radioligand. These data points were fit by linear regression with a slope of the line calculated at 2.53×10^7 M^{-1} s^{-1} and an intercept calculated at 0.000305 s^{-1}, yielding a calculated K_D of 12.05 pM.

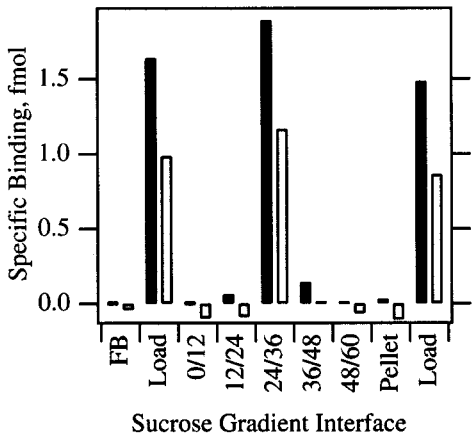

FIGURE 4: Co-localization of *D. melanogaster* head membrane [^{3}H]-IVM and [^{3}H]NAmide binding sites to membranes of similar densities. Fly head membranes were fractionated by centrifugation over a sucrose step gradient, and the fractions were assayed for specific binding sites for [^{3}H]IVM (solid bars) and [^{3}H]NAmide (open bars); the numbers below each fraction identify the interface: e.g., 12/24 was the interface of the 12 and 24% sucrose concentrations. As well, parallel tubes were carried though the binding assay without added membrane protein as a filter blank (FB) or with samples of the material loaded onto the sucrose gradient (Load). Based on the specific binding of each fraction and the binding in the material loaded onto the gradient and the volumes of each, 93% of the [^{3}H]IVM binding sites and 96% of the [^{3}H]-NAmide binding sites that were loaded onto the gradient were recovered. Similar results were achieved in two other experiments, all carried out in 1 mL assay volume at ligand concentrations of 0.12 and 0.2 nM for [^{3}H]IVM and [^{3}H]NAmide, respectively.

branes at that region of the gradient are enriched in these three neuronal markers.

Inhibition of NA Binding by GluCl Agonists. Since NA activates a glutamate-gated chloride channel (Figure 1C), we tested whether these channels are the high affinity binding site for this ligand in *D. melanogaster* head membranes. Consistent with this idea, we find that 1 mM L-glutamate decreases the affinity of [^{3}H]NAmide 3-fold (Figure 5A). This inhibition is attributable to the ability of L-glutamate to increase the dissociation rate of the [^{3}H]NAmide−receptor complex by 3-fold (Figure 5B). In an experiment similar to the time course of dissociation previously shown (Figure 3A), the time course of dissociation of [^{3}H]NAmide prebound to the receptor is measured by adding NA at 0.3 μM, without or with 1 mM L-glutamate or 1 μM IVM. IVM had no effect on the time course of dissociation of [^{3}H]NAmide. However, 1 mM L-glutamate decreases the half-time of dissociation from 24 to 10 min. Under all conditions, binding data for over 98% of the sites are fit by a single monoexponential decay curve (Figure 5B), which indicates that (within experimental error) all of the receptors for NA are allosterically coupled to a glutamate binding site. L-Glutamate is 100-fold more potent than D-glutamate; in a 2 h assay, L-glutamate has an EC_{50} for inhibiting [^{3}H]NAmide binding of 30 μM (data not shown). Ibotenate, a structurally constrained, poorly metabolized glutamate analogue, also shows this effect; 0.1 mM ibotenate decreases the half-time of dissociation of preformed [^{3}H]NAmide−receptor complexes by 3-fold from a half-time of 58 min under control conditions to a half-time of 20 min (Figure 3A). As would be predicted from the increase in the dissociation rate induced by ibotenate, the K_D for [^{3}H]NAmide is increased 3-fold in the presence of this compound (data not shown). When compared across experiments, the average fold increase in dissociation rate is 3.11 ± 0.29 (SEM, n = 5) with the addition of L-glutamate or ibotenate. In the experiment shown (Figure 5A), 1 mM glutamate did not change the B_{max} for [^{3}H]NAmide binding. However, in many membrane preparations, glutamate increases B_{max} by ca. 20%.

The NA and IVM Binding Sites Are Coupled. Interactions between the [^{3}H]NAmide binding sites and those for [^{3}H]-IVM were investigated using two types of experiments. First, inhibitor (either IVM or NA) was varied over 6 orders of

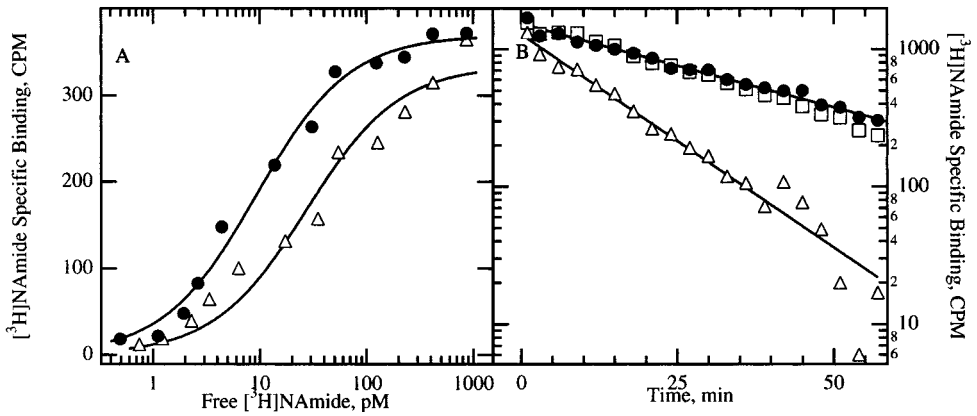

FIGURE 5: Glutamate increases the dissociation rate of the receptor−[^{3}H]NAmide complex. Panel A: Equilibrium binding of [^{3}H]NAmide to fly head membranes was measured in the absence (●) or in the presence of 1 mM L-glutamate (△) in a final volume of 0.95 mL with a receptor concentration of 14 pM. The K_D and B_{max} values that the data fit, in control and in 1 mM glutamate, were 9.3 and 27.3 pM and 370 and 335 CPM, respectively. Panel B: Fly head membranes were incubated with 80 pM [^{3}H]NAmide to equilibrium, and then dissociation of the receptor−ligand complex was followed by adding NA at 1 μM without (●) or with 1 mM L-glutamate (△), or with 0.1 μM IVM (□), followed by filtration at regular intervals thereafter. The lines in the right panel are linear regression fits to the data using a monoexponential function. The half-times calculated were 24 and 10 min for NA only and NA with L-glutamate, respectively. The half-time of dissociation is not significantly altered by the addition of IVM. Results are representative of 3 experiments.

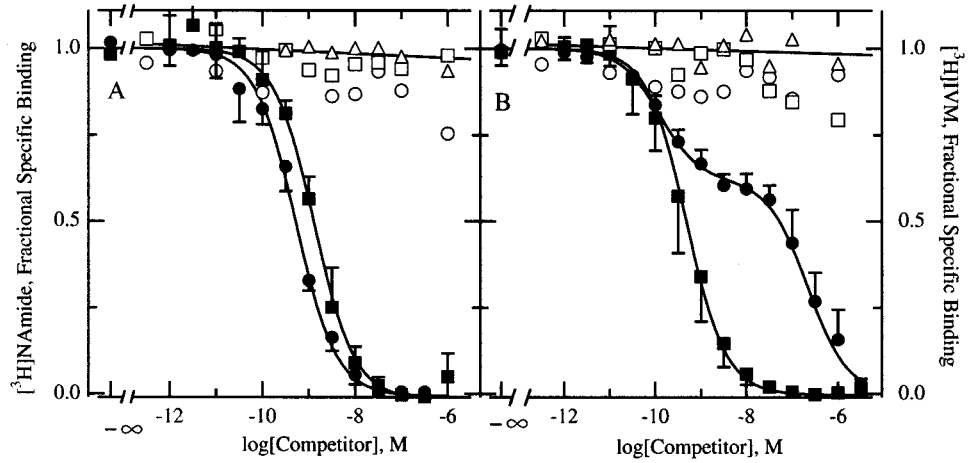

FIGURE 6: Molecular pharmacology of [^{3}H]NAmide binding to *D. melanogaster* head membranes. Membranes were incubated with [^{3}H]-NAmide (A) or [^{3}H]IVM (B) and the indicated concentrations of NA (●), IVM (■), the biologically inactive octahydro-IVM (□), the biologically inactive NA analogue 32β-hydroxymethyl NA (○, see Scheme 1 for the structure), or the structurally related indole diterpine paxilline (△) for typically 3 h. Using [^{3}H]NAmide as ligand, IVM had an IC_{50} of 1.3 nM, and NA had an IC_{50} of 0.5 nM. Using [^{3}H]IVM as ligand, IVM showed an IC_{50} of 0.5 nM; NA was modeled with a two-component binding model, with 40% of the receptors displaying an affinity of 0.125 nM and the remainder displaying an IC_{50} of 0.25 μM. This figure is the averaged result from 5 experiments for NA and IVM and from 1 experiment for paxilline, octahydro-IVM, and 32β-hydroxymethyl NA; the 5 experiments were carried out at ligand concentrations that ranged from 220 pM (initially) to 70 pM for [^{3}H]NAmide and from 120 to 33 pM for [^{3}H]IVM. The average maximal ligand bound was 22 and 26 pM for [^{3}H]NAmide and [^{3}H]IVM, respectively. The conversion factor from IC_{50} to K_I for the typical experiment was 5-fold for [^{3}H]IVM and 12-fold for [^{3}H]NAmide. If one uses this average value, the K_I values for IVM and NA inhibiting [^{3}H]NAmide binding were 108 and 42 pM. The K_I values for IVM and NA inhibiting [^{3}H]IVM binding were 100 pM, and 25 pM and 50 nM for K_H and K_L.

magnitude while [^{3}H]ligand (either [^{3}H]NAmide or [^{3}H]IVM) was maintained at a constant concentration (Figure 6). Second, the concentration of [^{3}H]ligand was varied over 2−3 orders of magnitude in the presence of fixed concentrations of the appropriate inhibitor (Figure 7).

Binding of [^{3}H]NAmide to fly head membranes is potently and completely inhibited by low concentrations of both NA and IVM (Figure 6A). The biologically inactive IVM analogue octahydro IVM (*6*) and the biologically inactive NA analogue 32β-hydroxymethyl NA (Scheme 1) do not inhibit binding of [^{3}H]NAmide, nor does the structurally related indole diterpene paxilline up to 1 μM (Figure 6A). Similar results were observed using [^{3}H]IVM as the ligand (Figure 6B); binding of [^{3}H]IVM was potently and completely inhibited by IVM, and affected by NA; again, the biologically inactive IVM or NA derivatives did not inhibit binding, nor did paxilline. Although the inhibition of [^{3}H]-IVM binding by IVM is consistent with a single high affinity binding site, the inhibition of [^{3}H]IVM by NA is more complex and is better described by two [^{3}H]IVM binding sites with differing affinities for NA. About half of the [^{3}H]-IVM binding is inhibited by NA with an IC_{50} of 0.12 nM, and the remainder is inhibited with an IC_{50} of 0.25 μM (Figure 6B); if one uses the average correction for competitive inhibition, then these IC_{50} values yield K_I values of 25 pM and 50 nM. This result suggests that [^{3}H]IVM binds to two different populations of receptors, that are differentiated by the potency of NA inhibition of binding.

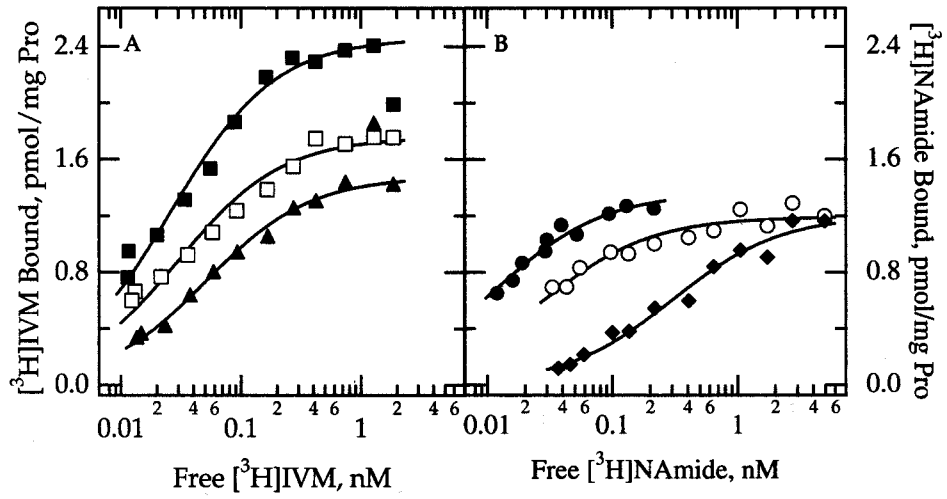

FIGURE 7: IVM and NA binding sites are coupled. Saturation binding isotherms were equilibrated overnight using [^{3}H]IVM (A) in the absence of (■) or presence of 1 nM NA (□), or 1 μM NA (▲), or (B) using [^{3}H]NAmide in the absence (●) or presence of 0.1 nM IVM (○), or 1 nM IVM (◆); all assays were carried out in a 1 mL volume using 12 μg of protein (15 pM receptor) for the [^{3}H]NAmide assay and 6 μg of protein (14 pM receptor) for the [^{3}H]IVM assay. The K_D and B_{max} values calculated for [^{3}H]IVM were respectively 26 pM and 2.46 pmol/mg of protein in the absence of NA, 29.5 pM and 1.76 pmol/mg of protein in the presence of 1 nM NA, and 51 pM and 1.48 pmol/mg in the presence of 1 μM NA. In the fitting for panel A, two data points were not included but are displayed; they are at the highest ligand concentration in the absence of NA and the penultimate highest concentration of ligand in the presence of 1 μM NA. For [^{3}H]-NAmide binding, the K_D and B_{max} values were 12 pM and 1.36 pmol/mg of protein in the absence of IVM, 28 pM and 1.19 pmol/mg of protein in the presence of 0.1 nM IVM, and 299 pM and 1.20 pmol/mg in the presence of 1 nM IVM. Converting the 0.1 and 1 nM IVM-induced changes in [^{3}H]NAmide K_D to a K_I for IVM by the relationship for competitive inhibition gives a 50 pM K_I for IVM. This figure is representative of the 3 times this type of experiment was carried out.

If the receptors for [^{3}H]IVM and for [^{3}H]NAmide are allosterically coupled and IVM can completely inhibit [^{3}H]-NAmide binding, but NA can potently inhibit only half of the binding sites for [^{3}H]IVM (Figure 6), then the site density for [^{3}H]IVM should be twice that for the high affinity [^{3}H]-NAmide binding site. This prediction was tested (Figure 7). When evaluated in the same membrane preparation, the B_{max} for [^{3}H]NAmide binding was 1.36 pmol/mg of protein, and the K_D was 12 pM (Figure 7B). The B_{max} for [^{3}H]IVM binding was nearly twice as large (2.46 pmol/mg of protein), and the K_D was 26 pM (Figure 7A). Thus, there are about twice as many binding sites for IVM as for NA in these fly head membranes.

Further evidence for an interaction between the IVM and NA binding sites is provided by saturation binding isotherms with each [^{3}H]ligand in the absence or presence of the other compound (Figure 7A,B). When measured in the presence of a concentration of NA that inhibits binding by 33% (1 nM; Figure 6B), the K_D of [^{3}H]IVM increased slightly, from a control value of 26 pM to 30 pM (Figure 7A). Inclusion of a concentration of NA that inhibits binding by 84% (1 μM; Figure 6B) further decreased the affinity by only about 2-fold to a K_D of 51 pM (Figure 7A). More importantly, these concentrations of NA decreased the B_{max} by 28 and 40%, respectively. The experiments shown in Figure 6B are directly comparable only to the binding data in Figure 7A for [^{3}H]IVM $\leq$120 pM. With [^{3}H]NAmide as the ligand, the presence of 0.1 nM IVM, a concentration that inhibits binding by 9% (Figure 6A), increases the K_D for [^{3}H]NAmide 3-fold from 9 to 28 pM with a modest decrease in B_{max} from 1.33 to 1.19 pmol/mg of protein. Inclusion of 1 nM IVM, the concentration that inhibits binding by 44%, increased the K_D an additional 10-fold to 0.3 nM, while changing insignificantly the B_{max} to 1.20 pmol/mg of protein. Although the apparent decrease in B_{max} for [^{3}H]IVM binding due to NA suggests that NA and IVM act at different sites on the same receptor, we cannot exclude the possibility that the B_{max} is unchanged and that NA causes a large change in K_D for half of the receptors (see Discussion). The lack of potent effect of NA on half of the IVM binding sites suggests that IVM binds to two different populations of receptors.

Thus far, we have established that the density of NA binding sites is about half the density of sites for IVM and that NA inhibits about half of the IVM binding with high affinity. There are two likely interpretations of these results; the first is that all binding is to a common supramolecular complex, with two binding sites for IVM and only one high affinity binding site for NA on this complex. Alternatively, there may be multiple different supramolecular complexes with high affinity for IVM, and only about half of these also serve as high affinity binding sites for NA. Studies of NA and IVM binding to other membrane preparations favor the idea that there are multiple supramolecular complexes with high affinity for IVM, but some are without high affinity sites for NA. Membranes isolated from *C. elegans*, grasshopper thoracic ganglia, grasshopper heads, grasshopper legs, or the lepidopteran *Spodoptera exigua*, all have readily detectable [^{3}H]IVM binding sites, but do not have high affinity binding sites for [^{3}H]NAmide. The limit of detection was 5% of total [^{3}H]IVM binding sites with a $K_D \leq 2$ nM. Likewise, 100 nM NA did not inhibit the binding of [^{3}H]-IVM to membranes isolated from *C. elegans* or grasshopper legs, suggesting that these IVM receptors are not coupled to a high affinity NA site. Purified synaptic plasmalemmal membranes prepared from rat cortex also have high affinity binding sites for [^{3}H]IVM (*4*), but this binding is not inhibited by 1 μM NA and no high affinity binding of [^{3}H]NAmide is detectable; the limit of detection was 5% of the total [^{3}H]-IVM binding sites with a $K_D \leq 2$ nM. The high affinity [^{3}H]-NAmide binding site is found in membranes from two other

dipterans, *Musca domestica* and *Lucilia sericata* (data not shown). In grasshopper ganglia and head membranes, binding of IVM is inhibited by NA with an IC_{50} of 10 nM (data not shown). Although high affinity [^{3}H]NAmide binding sites are abundant in membranes from heads of adult *Drosophila*, they are not found in membranes isolated from larvae, even though ample [^{3}H]IVM binding sites are present. Thus, [^{3}H]-IVM binding sites consist of multiple types that differ in affinity for NA, and the binding site for [^{3}H]NAmide may be developmentally regulated.

DISCUSSION

In this study, we have characterized a new insecticidal agent, nodulisporic acid, that has a mechanism of action similar to that of ivermectin, but a more restricted range of activity. Both nodulisporic acid and ivermectin activate glutamate-gated chloride channels. High affinity binding sites for ivermectin have been identified in nematodes, insects, and mammals, while those for nodulisporic acid have only been found in some dipterans. We have altered the protocol used to characterize IVM binding and find that this ligand binds with higher affinity than previously recognized (K_D = 25 pM). Nodulisporic acid binds with comparable potency (K_D = 12 pM). Although analysis of saturation IVM binding is consistent with a single population of high affinity sites, studies with NA indicate that IVM binds to several types of receptors with similar affinities.

High affinity binding of [^{3}H]NAmide to *Drosophila melanogaster* head membranes appears to represent 1 to 1 binding to an apparent single receptor because the same K_D is obtained by equilibrium measurements (Figure 2) and from the ratio of association and dissociation rates (Figure 3), and because the dissociation of ligand is monoexponential for ≥98% of the sites (Figures 3A and 5B). However, the binding of [^{3}H]IVM to *C. elegans* membranes also appeared to be to a single site (*4*, *28*), while knock-out or loss-of-function mutations indicate high affinity binding to three different GluCl α-subunits (*9*). Nevertheless, the dissociation kinetics and the inhibition of [^{3}H]NAmide binding by IVM (Figures 6A and 7B), glutamate (Figure 5), and ibotenate (Figure 3A) are all consistent with high affinity binding to a single type of GluCl or multiple GluCls with similar affinities (*33*) and dissociation rates of NA. Both L-glutamate and ibotenate increase the rate of dissociation of NA about 3-fold, indicating that NA binds at a site distinct from these GluCl activators. All [^{3}H]NAmide binding sites are associated with GluCls because >98% of the [^{3}H]NAmide binding is inhibited by glutamate (Figure 5B) and ibotenate (Figure 3A). This interpretation is supported by electrophysiological studies showing that NA is an activator of grasshopper glutamate-gated chloride channels (Figure 1A,C).

NA and IVM also activate homomultimers of *Drosophila* GluCl expressed in *Xenopus* oocytes (*11*, *34*: NA is identified as compound **1** in the latter). However, the pharmacology of NAmides in this heterologous expression system is inconsistent with that of native grasshopper GluCl, [^{3}H]NAmide binding to this preparation is inconsistent with binding to *Drosophila* head membranes, and some analogues of NA with insecticidal activity do not activate these homomultimers (M.M.S., V.A.W., R.M.B., and C.J.C., unpublished observations).

The dissociation constants for [^{3}H]NAmide (9−12 pM) and [^{3}H]IVM (25 pM) indicate that these compounds are among the most potent known ligands for ligand-gated ion channels. Some of the biological effects of IVM in nematode and crayfish are consistent with this binding affinity (*12*, *35*). However, the electrophysiological effects of IVM in grasshopper neurons are less potent than expected from the ligand binding affinity. The concentration−response relationship for IVM is difficult to assess with grasshopper motorneurons because the responses to IVM across cells are not uniform. In some experiments (e.g., Figure 1D, right side), 10 nM IVM-PO_4 was maximally effective, but in other experiments, higher concentrations were needed to achieve maximal current activation. The minimally effective concentration of IVM-PO_4 was about 1 nM in most experiments, and the potency was similar when IVM-PO_4 was tested in combination with glutamate. However, IVM-induced channel opening can greatly underestimate the affinity of drug for its receptor. At low concentrations of agonist, channel opening should be extremely slow, and desensitization can prevent accumulation of channels in an open state. In addition, the equilibrium binding assay is an overnight incubation, which allows for equilibration of slow binding ligands, whereas the electrophysiological experiments may well last less than an hour.

The [^{3}H]NAmide binding site is coupled to an [^{3}H]IVM binding site in a complex fashion. First, the two sites co-localize by a low-resolution technique to membranes of a similar density (Figure 4) and to a location where another neuronal membrane marker, [^{3}H]saxitoxin binding to sodium channels, segregates; co-localization perforce is required if the sites are coupled. Second, IVM inhibits [^{3}H]NAmide binding with an IC_{50} of 1.3 nM (Figure 5A); correcting that IC_{50} to a K_I by using the correction factor for competitive inhibition (for the typical experiment) gives a K_I of about 0.1 nM (Figure 6A). Similarly, IVM inhibits [^{3}H]NAmide binding in an apparently competitive fashion in saturation binding isotherm experiments (Figure 7B): 100 pM IVM shifts the K_D for [^{3}H]NAmide 3-fold, and increasing the IVM concentration 10-fold shifts the K_D by an additional 10-fold. These data imply a K_I for IVM inhibition of [^{3}H]NAmide binding of 30−50 pM and are consistent with a purely competitive interaction of overlapping binding sites. Finally, however, NA inhibits binding of [^{3}H]IVM with two distinct affinities: a K_H of 25 pM for 40% of the sites and a K_L of 50 nM for the remainder (K_I values were calculated as above from IC_{50}'s of 125 pM and 0.25 μM, Figure 6B). The K_D for direct binding of [^{3}H]NAmide is 9−12 pM (Figures 2, 3, and 7).

One explanation for the interaction between NA and IVM is that both ligands bind to GluCls with high affinity, but about half of the IVM binding sites are to a different binding site on the same channel or to a different type of channel that does not have a high affinity binding site for NA. The latter interpretation predicts that the fraction of IVM binding susceptible to high affinity inhibition by NA will vary among tissue preparations; studies with membranes from grasshoppers, *Drosophila* embryos, and *C. elegans* are consistent with this prediction. The electrophysiological studies with grasshopper neurons suggests that there are GluCls that bind IVM with high affinity, but not NA. These neurons have a high density of IVM binding sites (*10*) and large glutamate-gated

chloride currents (Figure 1), but lack the picomolar affinity binding sites for NA. In all our studies, we have not found a preparation that binds [^{3}H]NAmide without a corresponding binding site for [^{3}H]IVM or responds to NA but not to IVM.

Although some of our studies indicate the existence of receptors that bind with high affinity IVM but not NA, it is possible that these are not present in *Drosophila* head membranes and that this preparation has a single receptor for both NA and IVM. This explanation requires that the receptor has multiple high affinity binding sites for IVM but not for NA and that NA inhibits IVM binding to only half of the IVM binding sites with high potency. The simplest formulation of this interpretation is that NA competitively inhibits the binding of IVM, but only at one of its two binding sites on a GluCl with high potency. The inhibition of [^{3}H]NAmide binding by IVM (Figure 7B) is consistent with such a competitive interaction. Since the two molecules have no gross structural similarity, their binding sites are likely overlapping but nonidentical. This explanation also predicts that NA will alter the apparent K_D for IVM binding, but not the B_{max}. Although an apparent change in B_{max} is shown in Figure 7A, it is not feasible to use high enough concentrations of [^{3}H]IVM to definitively rule out a NA-induced change in the K_D of [^{3}H]IVM for half of the binding sites. It is possible to account for these binding data with competitive inhibition by NA with two distinct affinities: high affinity binding sites with $K_I = 25$ pM for half of the sites and low affinity binding sites with $K_I = 50$ nM for the remainder. The K_I for high affinity inhibition is consistent with the K_D for NA of 9−12 pM obtained from direct binding experiments (Figures 2, 3, and 7B), supporting the interpretation of a competitive interaction. Interestingly, both the control binding isotherm of [^{3}H]IVM (Figure 7A) and the binding isotherms previously presented (*10*) are compatible with ligand binding to a single site and do not indicate multiple populations of receptors. Thus, the multiple [^{3}H]-IVM binding sites must have very similar affinities for IVM (*33*).

We are biochemically isolating IVM receptors to determine whether all IVM binding sites are on the same complex or are on multiple complexes that are biochemically and immunologically distinct. We find that the multimer containing both the [^{3}H]IVM and [^{3}H]NAmide high affinity binding sites contains both *Drosophila* GluCl (*11*) and a subunit of GABA-gated chloride channels corresponding to the resistance to dieldrin and lindane (*rdl*) locus (*36*−*39*). The IVM binding sites associated with low affinity NA binding contain GluCl but not Rdl (*37*−*39*).

In the membrane fragments and vesicles used in the binding assay, GluCls can be in the closed, open, or desensitized states. Although the distribution among these states is unknown, it is likely that channels flicker among these states. We hypothesize that in the absence of any agonist, most channels are in the closed, available state and that L-glutamate shifts channels to the desensitized state. Thus, the inhibition of NA binding by glutamate (Figures 3A and 5A,B) suggests that NA binds with greater affinity to closed-available channels than to desensitized ones. Based on microscopic reversibility, we therefore expect that NA inhibits glutamate-induced desensitization. Indeed, NA potentiates glutamate-induced channel opening (Figure 1C) and, at higher concentrations, opens the channel alone (Figure 1A,C,D). In *C. elegans*, opening of the GluCl channel by IVM leads to paralysis, starvation, and death of the organism (*8*). In this work, we show that NA has a similar effect on insect GluCl.

NA is a remarkable example of convergent evolution. The avermectins are bacterial products that open GluCls. Until now, the only other agents known to target GluCls were close structural analogues such as the milbemycins, which also are bacterial products. NA is produced by an endophytic fungus (*17*) and is grossly structurally dissimilar from the avermectins, yet it also opens GluCls. The discovery of additional natural products that target GluCls reinforces the belief that opening GluCls is an efficacious means of achieving insecticidal activity. NA, then acts as a natural defense against foraging insects and is thus an excellent molecule for an endophydic fungus to produce.

ACKNOWLEDGMENT

We thank the following colleagues at Merck: E. Hayes for suggesting the use of bacitracin in the binding assay; Y. Wang and J. Warmke for culturing *D. melanogaster*; O. McManus and L. Helms for Maxi-K channel studies; J. Arena and K. Liu for oocyte studies; R. Slaughter and J. Felix for Ca and K_V1.X channel studies; S. Koprak for intracranial injections; T. Chen, J. Tkacz, and J. Ondeyka for supplies of 32β-hydroxymethyl NA; W. Shoop for insecticidal studies; and M. L. Garcia and A. Smith for discussions after reading the manuscript. We thank John Capinera and Jason Squirtier (Department of Entomology and Nematology, University of Florida at Gainesville) and Douglas Streett and Mary Swan (Rangeland Insect Laboratory, Montana State University, Bozeman, MT) for generously supplying adult *Schistocerca americana*.

REFERENCES

1. Vassilatis, D. K., Elliston, K. O., Paress, P. S., Hamelin, M., Arena, J. P., Schaeffer, J. M., Van der Ploeg, L. H., and Cully, D. F. (1997) *J. Mol. Evol. 44*, 501−508.
2. Campbell, W. (1989) *Ivermectin and Abamectin*, Springer-Verlag, New York.
3. Fisher, M., and Mrozik, H. (1992) *Annu. Rev. Pharmacol. Toxicol. 32*, 537−553.
4. Schaeffer, J. M., and Haines, H. W. (1989) *Biochem. Pharmacol. 38*, 2329−2338.
5. Arena, J. P., Liu, K. K., Paress, P. S., Schaeffer, J. M., and Cully, D. F. (1992) *Brain Res. Mol. Brain Res. 15*, 339−348.
6. Arena, J. P., Liu, K. K., Paress, P. S., Frazier, E. G., Cully, D. F., Mrozik, H., and Schaeffer, J. M. (1995) *J. Parasitol. 81*, 286−294.
7. Cully, D. F., Vassilatis, D. K., Liu, K. K., Paress, P. S., Van der Ploeg, L. H., Schaeffer, J. M., and Arena, J. P. (1994) *Nature 371*, 707−711.
8. Dent, J. A., Davis, M. W., and Avery, L. (1997) *EMBO J. 16*, 5867−5879.
9. Dent, J. A., Smith, M. M., Vassilatis, D. K., and Avery, L. (2000) *Proc. Natl. Acad. Sci. U.S.A. 97*, 2674−2679.
10. Rohrer, S. P., Birzin, E. T., Costa, S. D., Arena, J. P., Hayes, E. C., and Schaeffer, J. M. (1995) *Insect Biochem. Mol. Biol. 25*, 11−17.
11. Cully, D. F., Paress, P. S., Liu, K. K., Schaeffer, J. M., and Arena, J. P. (1996) *J. Biol. Chem. 271*, 20187−20191.
12. Brownlee, D. J., Holden Dye, L., and Walker, R. J. (1997) *Parasitology 115*, 553−561.
13. Holden Dye, L., and Walker, R. J. (1990) *Parasitology 101 Pt. 2*, 265−271.

14. Walker, R. J., Colquhoun, L., and Holden Dye, L. (1992) *Acta Biol. Hung. 43*, 59−68.
15. Cole, L. M., Roush, R. T., and Casida, J. E. (1995) *Life Sci. 56*, 757−765.
16. Bermudez, I., Hawkins, C. A., Taylor, A. M., and Beadle, D. J. (1991) *J. Recept. Res. 11*, 221−232.
17. Ondeyka, J. G., Helms, G. L., Hensens, O. D., Goetz, M. A., Zink, D. L., Tsipouras, O. D., Shoop, W. L., Slayton, L., Dombrowski, A. W., Polishook, J. D., Ostlind, D. A., Tspi, N. N., Ball, R. G., and Somgj, S. B. (1995) *J. Am. Chem. Soc. 119*, 8809−8816.
18. Ostlind, D. A., Felcetto, T., Misura, A., Ondeyka, J., Smith, S., Goetz, M., Shoop, W., and Mickle, W. (1997) *Med. Vet. Entomol. 11*, 407−408.
19. Dowd, P. F., Cole, R. J., and Vesonder, R. F. (1988) *J. Antibiot. 41*, 1868−1872.
20. Prestidge, R. A., and Gallagher, R. T. (1988) *Ecol. Entomol. 13*, 429−435.
21. Yao, Y., Peter, A. B., Baur, R., and Sigel, E. (1989) *Mol. Pharmacol. 35*, 319−323.
22. Knaus, H. G., McManus, O. B., Lee, S. H., Schmalhofer, W. A., Garcia-Calvo, M., Helms, L. M., Sanchez, M., Giangiacomo, K., Reuben, J. P., and Smith, A. B., III (1994) *Biochemistry 33*, 5819−5828.
23. Benson, J. (1992) *J. Exp. Biol. 170*, 203−233.
24. Bermudez, I., Beadle, D., and Benson, J. (1992) *J. Exp. Biol. 165*, 43−60.
25. Ertel, E. A., Warren, V. A., Adams, M. E., Griffin, P. R., Cohen, C. J., and Smith, M. M. (1994) *Biochemistry 33*, 5098−5108.
26. Pearson, H., Lees, G., and Wray, D. (1993) *J. Exp. Biol. 177*, 201−221.
27. Suter, C., and Usherwood, P. N. R. (1985) *Comp. Biochem. Physiol. 80C*, 221−229.
28. Cully, D. F., and Paress, P. S. (1991) *Mol. Pharmacol. 40*, 326−332.
29. Feigenbaum, P., Garcia, M. L., and Kaczorowski, G. J. (1988) *Biochem. Biophys. Res. Commun. 154*, 298−305.
30. Usherwood, P. (1994) *Adv. Insect Physiol. 24*, 309−341.
31. Felix, J. P., Bugianesi, R. M., Schmalhofer, W. A., Borris, R., Goetz, M. A., Hensens, O. D., Bao, J. M., Kayser, F., Parsons, W. H., Rupprecht, K., Garcia, M. L., Kaczorowski, G. J., and Slaughter, R. S. (1999) *Biochemistry 38*, 4922−4930.
32. Garcia Calvo, M., Leonard, R. J., Novick, J., Stevens, S. P., Schmalhofer, W., Kaczorowski, G. J., and Garcia, M. L. (1993) *J. Biol. Chem. 268*, 18866−18874.
33. DeLean, A., Handcock, A. A., and Lefkowitz, R. J. (1982) *Mol. Pharmacol. 21*, 5−16.
34. Cully, D. F., Arena, J. P., Paress, P. S., and Liu, K. K. (1997) in US Patent 5 693 492.
35. Zufall, F., Franke, C., and Hatt, H. (1989) *J. Exp. Biol. 142*, 191−205.
36. ffrench-Constant, R. H., Rocheleau, T. A., Steichen, J. C., and Chalmers, A. E. (1993) *Nature 363*, 449−451.
37. Warren, V. A., Thomas, B. S., Dean, D., Wallace, M., Leonard, R. J., Kaczorowski, G. J., and Smith, M. M. (1999) *Soc. Neurosci. Abstr. 25*, 1484.
38. Ludmerer, S. W., Zheng, Y., Hirschberg, B., Smith, M. M., and Cully, D. (1999) *Soc. Neurosci. Abstr. 25*, 1484.
39. Smith, M. M., Thomas, B. S., Warren, V. A., Brochu, R., Dick, I., Hirschberg, B., Arena, J., Ludmerer, S. W., Zheng, Y., Cully, D., and Cohen, C. J. (1999) *Soc. Neurosci. Abstr. 25*, 1483.

BI992943I